Materials Letters 278 (2020) 128468

Contents lists available at ScienceDirect

Materials Letters

journal homepage: www.elsevier.com/locate/mlblue

Amorphous carbon to graphene: Carbon diffusion via nickel catalyst

Hanchao Li [a,b], Diwei Shi [b,d], Peng Guo [a], Jing Wei [a,c], Ping Cui [a,b], Shiyu Du [d,*], Aiying Wang [a,c,*]

[a] Key Laboratory of Marine Materials and Related Technologies, Zhejiang Key Laboratory of Marine Materials and Protective Technologies, Ningbo Institute of Materials Technology and Engineering, Chinese Academy of Sciences, Ningbo 315201, China
[b] School of Physical Science and Technology, ShanghaiTech University, Shanghai 201210, China
[c] Center of Materials Science and Optoelectronics Engineering, University of Chinese Academy of Sciences, Beijing 100049, China
[d] Engineering Laboratory of Advanced Energy Materials, Ningbo Institute of Materials Technology and Engineering, Chinese Academy of Sciences, Ningbo 315201, China

ARTICLE INFO

Article history:
Received 14 March 2020
Received in revised form 20 July 2020
Accepted 3 August 2020
Available online 5 August 2020

Keywords:
Amorphous carbon
Carbon materials
Grain boundaries
Nickel-induced crystallization

ABSTRACT

Graphene can be synthesized via metal catalysis using solid carbon source. In this paper, graphene was fabricated using amorphous carbon. We further elucidated the process of carbon diffusion and graphene formation at low temperatures using a comprehensive experimental and theoretical strategy. The diffusion barrier of carbon in nickel crystal is different from that of carbon along nickel grain boundaries, resulting in that the layer of graphene is uncontrollable. Based on our findings, we identified the causes of graphene heterogeneity and the process of carbon diffusion.

1. Introduction

Graphene, has aroused great interest among the scientists owing to its unique structure and excellent properties [1,2]. Previous study has reported graphene synthesis by solid carbon source, which showed the controllability and simplicity of the process [3]. Amorphous carbon (a-C), as one allotrope of carbon, is a kind of solid carbon source. It gains much attention in graphene synthesis because the preparation is simple and the film is uniform [4,5].

In previous researches, the carbon source and Ni/C ratios are discussed in detail [6,7]. It was found that high density a-C is inclined to form graphene and Ni/C ratios affect the diffusion of carbon in nickel, resulting in the change of graphene growth. The calculation and experiment results showed that the graphene formation can be conveyed by an equation containing Ni/C ratios and is mainly dominated by the diffusion of carbon. Nevertheless, the detailed diffusion process of carbon is not revealed yet, and it is necessary to understand the detailed diffusion mechanism of carbon via nickel catalyst. Thus, in this study, we focus on the carbon diffusion process during graphene formation from amorphous carbon via nickel catalyst. With experimental results and simulation calculations, we shed light on the reasons for non-uniformity of graphene. The important result is that the diffusion barrier of carbon in nickel interspace and carbon along nickel grain boundaries (GBs) is different.

2. Experimental

P-type Si (100) wafers coated with 300 nm SiO_2 (SiO_2/Si) were applied as substrates. Based on previous simulation results [6], a-C of about 2–4 nm was deposited on substrates and the nickel layer of 80 nm was deposited on a-C. For the detailed process and schematic information, refer to Ref [5].

After deposition process, the sample was annealed at 500 °C with a pressure below 10^{-2} Pa in a quartz tube (MTI-OTF-1200X) for annealing experiments. The heating rate was 100 °C/min and annealing time was 1, 3 and 5 h, respectively. The evolution of microstructure was revealed by transmission electron microscopy (TEM, FEI Tecnai F20 200 kV). First principles calculations based on the density functional theory (DFT) with a cutoff energy of 360 eV were used in this paper. The diffusion barrier of carbon in nickel was calculated in conjunction with the climbing image nudged elastic band method which was implemented in VASP [8,9]. The generalized gradient approximation (GGA) function with the scheme of Perdew-Burke-Ernzerhof was employed for exchange and correlation energy [10,11]. Periodic boundary conditions were performed during calculation. In this work, a four layers slab (each

* Corresponding authors at: Engineering Laboratory of Advanced Energy Materials, Ningbo Institute of Materials Technology and Engineering, Chinese Academy of Sciences, Ningbo 315201, China (S. Du); Key Laboratory of Marine Materials and Related Technologies, Zhejiang Key Laboratory of Marine Materials and Protective Technologies, Ningbo Institute of Materials Technology and Engineering, Chinese Academy of Sciences, Ningbo 315201, China (A. Wang).

E-mail addresses: dushiyu@nimte.ac.cn (S. Du), aywang@nimte.ac.cn (A. Wang).

https://doi.org/10.1016/j.matlet.2020.128468
0167-577X/

layer has 16 Ni atoms) was adopted to simulate the carbon diffusion along Ni (1 1 1) GBs. The supercell of 2 × 2 × 2 fcc-Ni (32 atoms) and a C atom, namely Ni32C, is large enough to avoid the interactions between C and neighbor C atoms considering periodic boundary condition [12]. Thus, Ni32C was modeled to calculate the diffusion barrier of an isolated carbon atom in Ni interstice.

3. Result and discussion

The structure of as-deposited sample is shown in Fig. 1(a). The embedded images in Fig. 1(b) are the distribution of elements within the rectangular area. Thereby the bilayer structure of the Ni/a-C specimen with Ni top layer and a-C bottom layer was fabri-

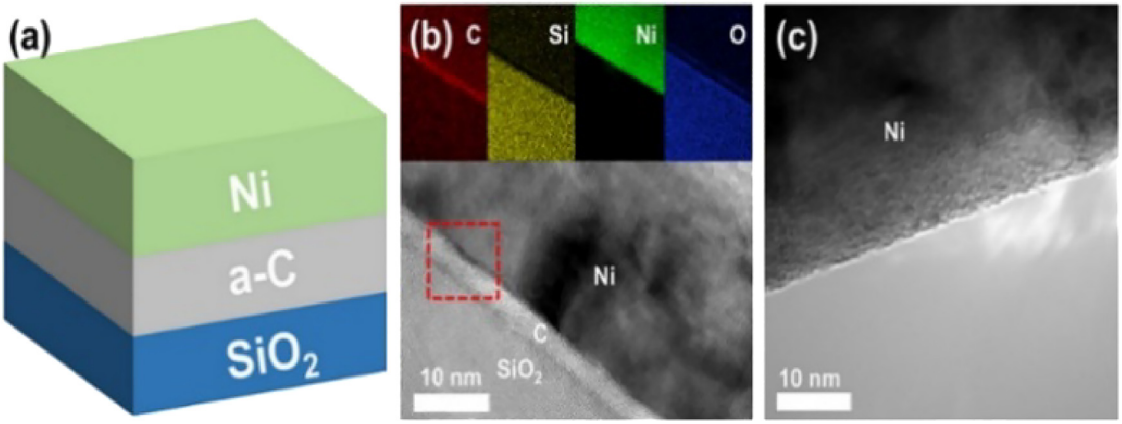

Fig. 1. The schematic of as-deposited sample (a). The microstructure of as-deposited sample and distribution of elements (b). The microstructure of nickel surface after sample was annealed at 500 °C for 1 h (c).

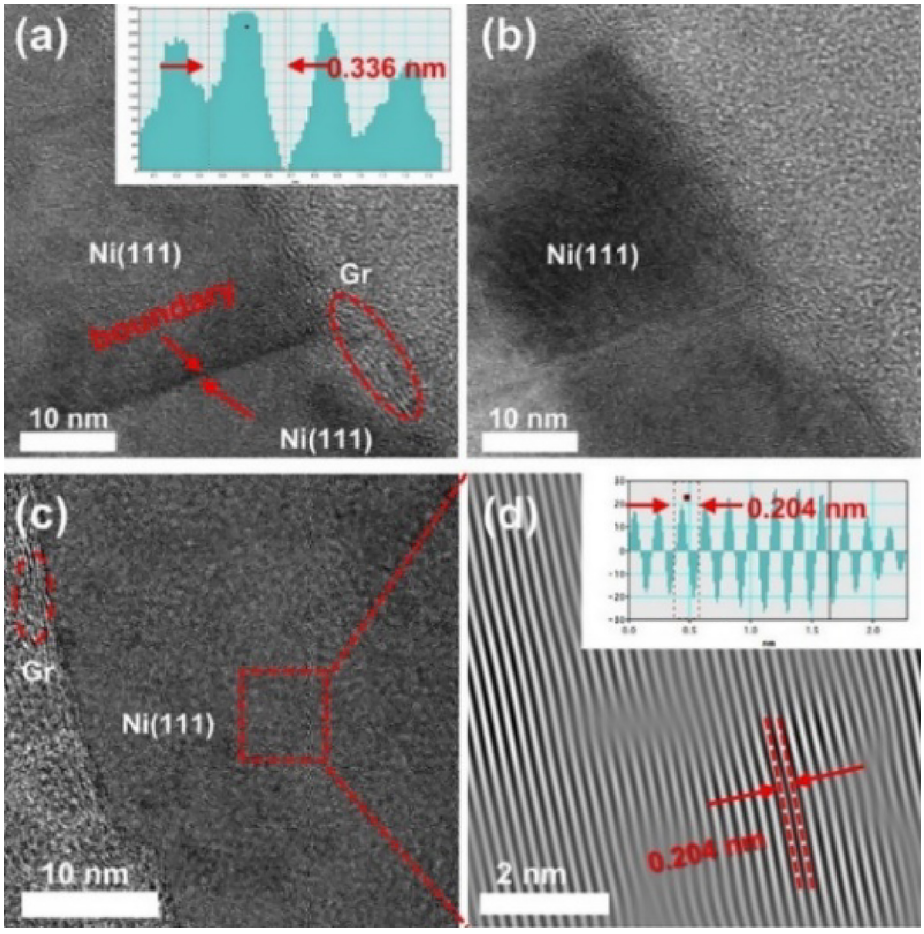

Fig. 2. The microstructure of nickel surface at GBs site (a) and nickel grain surface (b) after sample was annealed at 500 °C for 3 h. (c) Graphene (Gr) on the nickel surface after sample was annealed at 500 °C for 5 h. (d) The Ni (1 1 1) microstructure of the rectangular area in (c).

Table 1
Diffusion barrier and distance in calculation.

	GB-front	GB-rotate	tetrahedral interstice to neighboring tetrahedral interstice	octahedral interstice to neighboring octahedral interstice	tetrahedral interstice toneighboring octahedral interstice
Barrier (eV)	0.71	0.18	0.75	2.9	3.6
Distance (Å)	2.5	2.5	1.8	2.5	1.5

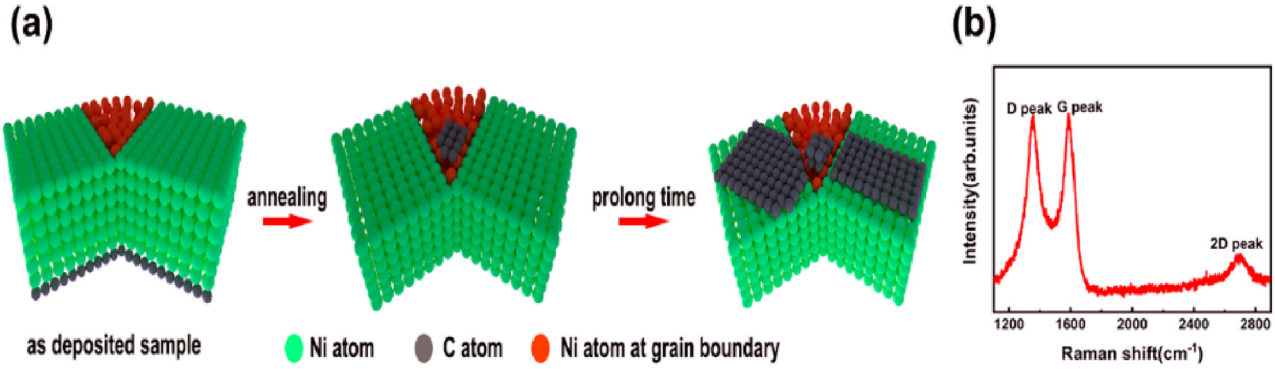

Fig. 3. (a) The schematic of carbon diffusion and graphene formation. (b) The Raman spectra of sample after annealed at 500 °C for 5 h.

cated successfully. After annealing at 500 °C for 1 h, carbon dissolved into nickel resulting in no obvious signal of carbon enrichment between SiO_2 and Ni. In addition, there was no evident a-C and graphene on nickel surface (Fig. 1(c)), which was in agreement with previous results [5]. When the annealing time was extended to 3 h, carbon segregated on nickel surface along nickel GBs (Fig. 2(a)). The inter-planar space of carbon was 0.336 nm, indicating that graphene was formed at the nickel GBs site [5,13]. However, there was no graphene on nickel grain surface as can be seen from Fig. 2b. The previous research showed that there is a diffusion mixed layer of carbon and nickel [6,7]. However, we cannot find evidence in Fig. 2(a), (b). Further, the graphene was found on nickel grain surface while annealing time was extended to 5 h (Fig. 2(c)). We deduced that carbon diffuses along nickel boundary preferentially.

Based on the first principles, the diffusion paths and barrier of carbon atom along GBs of Ni (1 1 1) were calculated. The existence of Ni (1 1 1) crystal plane has been proved owing to its inter-planar spacing 0.204 nm (Fig. 2(d)). In our simulation, 2 layers of Ni (1 1 1) plane were intercepted from the fcc-Ni (16 Ni atoms in each layer). Two groups of them were connected to each other as the grain boundary (4 layers of Ni (1 1 1) and 64 Ni atoms in total) by some docking method. Upper two layers are named surface A, and lower two layers are named surface B, both of which have the same structure. The simulation results show that there are two most stable docking forms: GB-front and GB-rotate.

The adhesion energy is calculated by formula: Wad = Ea + Eb-Ea/b, where Ea and Eb are the energy of the surface A and surface B, respectively. Ea/b is the total energy of the system of A/B interface. The values of adhesion energy for GB-front and GB-rotate are 6.8 eV and 15.5 eV, respectively. The value of adhesion energy above zero indicates the stability of the interface connection. Hence both two systems of GBs are relatively stable and the interface adhesive strength is higher for GB-rotate. We introduce an additional C atom in GB-front and GB-rotate to simulate the diffusion of C atom along Ni GBs and the diffusion process is sketched in Fig. S1 (a) and (b). The C atom in the configurations of GB-front and GB-rotate interacted with the nearest 4 layers of Ni atoms, and the influence on C atom from excess layers of Ni atoms could be negligible.

Carbon diffusion in nickel interstice includes three means:
1. one tetrahedral interstice to another tetrahedral interstice;
2. one octahedral interstice to another octahedral interstice;
3. one tetrahedral interstice to another octahedral interstice

(The simulation diffusion process of carbon in nickel interstice is given in Fig. S2, 3, 4.). Three diffusion paths are all designed between the two nearest neighboring interstitial positions.

Table 1 summarizes the results of calculation simulations about the diffusion barrier and distance. The diffusion barriers of three different paths in nickel interstice were 0.75 eV, 2.9 eV, 3.6 eV, which are higher than carbon along Ni (1 1 1) GBs, indicating that the diffusion of carbon will be more affected by the Ni (1 1 1) GBs. Thus, carbon will diffuse along nickel GBs preferentially. Zhu [12] calculated the heat of solution of carbon atom in nickel matrix and found that surface diffusion process is dominated compared to bulk diffusion. Thus, the carbon will diffuse along nickel surface when carbon atoms reach nickel surface despite that the bulk diffusion is existing.

Owing to low diffusion barrier of carbon along nickel GBs, carbon will segregate at the nickel GBs site preferentially during annealing. To lower the energy of system, graphene is formed on nickel surface due to metal-induced and diffusion-assisted mechanism [14]. Thus, there is no graphene or carbon residue between Ni and SiO_2. With increasing annealing time, carbon segregates from nickel along nickel GBs further and graphene grows, covering not only the GBs site but also nickel grain surface [13] as is shown in Fig. 3 (a). The Raman spectra was measured to evaluate the quality of graphene. However, the quality of graphene is not very well (Fig. 3 (b)), which should be improved and will be discussed in future research.

4. Conclusion

In this work, carbon diffusion and graphene formation were discussed in detail by experiments and simulations. The diffusion barrier of carbon along nickel GBs is lower than that of carbon from nickel grains interstice. Carbon diffuses along nickel GBs and graphene is formed on nickel GBs preferentially. With increasing annealing time, to lower the energy of system, carbon diffuses along the nickel grain and covers the surface of nickel in the form

of graphene. These results imply that the graphene formation mechanism is diffusion-assisted and metal-induced. Our data shed light on the effects of GBs during graphene formation, which provide new insights into graphene synthesis.

CRediT authorship contribution statement

Hanchao Li: Conceptualization, Methodology, Software, Data curation, Formal analysis, Writing - original draft, Writing - review & editing. **Diwei Shi:** Methodology, Software, Writing - review & editing. **Peng Guo:** Data curation, Formal analysis. **Jing Wei:** Software, Data curation. **Ping Cui:** Writing - review & editing. **Shiyu Du:** Resources, Validation, Supervision. **Aiying Wang:** Resources, Writing - review & editing, Supervision, Project administration, Funding acquisition.

Declaration of Competing Interest

The authors declare that they have no known competing financial interests or personal relationships that could have appeared to influence the work reported in this paper.

Acknowledgements

This work was financially supported by the K.C.Wong Education Foundation (GJTD-2019-13), the A-class pilot of the Chinese Academy of Sciences (XDA22010303), the Ningbo Science and Technology Innovation Project (2018B10014). We thank Dr Zhenyu Wang from Ningbo Institute of Materials Technology and Engineering for his help in transmission electron microscopy sample preparation.

Appendix A. Supplementary data

Supplementary data to this article can be found online at https://doi.org/10.1016/j.matlet.2020.128468.

References

[1] K.S. Novoselov, A.K. Geim, S.V. Morozov, D. Jiang, Y. Zhang, S.V. Dubonos, I.V. Grigorieva, A.A. Firsov, Science 306 (2004) 666–669.
[2] M.A. Kim, N.X. Qiu, Z.T. Li, Q. Huang, Z.F. Chai, S.Y. Du, H.T. Liu, Adv. Funct. Mater. 30 (2020) 1909269.
[3] Z. Sun, Z. Yan, J. Yao, E. Beitler, Y. Zhu, J.M. Tour, Nature 468 (2010) 549–552.
[4] B.S. Nguyen, J.F. Lin, D.C. Perng, Appl. Phys. Lett. 106 (2015) 221604.
[5] H.C. Li, X.W. Li, J. Wei, Z.Y. Wang, P. Guo, P.L. Ke, H. Saito, P. Cui, A.Y. Wang, Diam. Relat. Mater. 101 (2020) 107556.
[6] X.W. Li, Z.Y. Wang, H.C. Li, A.Y. Wang, K.R. Lee, J. Phys. Chem. C 123 (2019) 27834–27842.
[7] X.W. Li, Y. Zhou, X.W. Xu, A.Y Wang, K.R. Lee, Phys. Chem. Chem. Phys., 21 (2019)9384-9390
[8] G. Henkelman, B. Uberuaga, H. Jónsson, J. Chem. Phys. 113 (2000) 9901–9904.
[9] G. Kresse, J. Furthmüller, Phys. Rev. B 54 (1996) 169–186.
[10] J.P. Perdew, K. Burke, M. Ernzerhof, Phys. Rev. Lett. 77 (1996) 3865.
[11] M. Ernzerhof, G. Scuseria, J. Chem. Phys. 110 (1999) 5029–5036.
[12] Y.A. Zhu, Y.C. Dai, D. Chen, W.K. Yuan, Carbon 45 (2007) 21–27.
[13] C.M. Seah, S.P. Chai, A.R. Mohamed, Carbon 70 (2014) 1–21.
[14] Y.Y. Chen, J.Y. Wang, P. Schützendübe, Z.M. Wang, E.J. Mittemeijer, Carbon 159 (2020) 37–44.